RSC Advances

This is an *Accepted Manuscript*, which has been through the Royal Society of Chemistry peer review process and has been accepted for publication.

Accepted Manuscripts are published online shortly after acceptance, before technical editing, formatting and proof reading. Using this free service, authors can make their results available to the community, in citable form, before we publish the edited article. This *Accepted Manuscript* will be replaced by the edited, formatted and paginated article as soon as this is available.

You can find more information about *Accepted Manuscripts* in the **Information for Authors**.

Journal Name

ARTICLE

Three-Dimensional Graphene Nanosheets/Carbon Nanotube Paper as Flexible Electrodes for Electrochemical Capacitors

Xiaoliang Yun, Jie Wang, Laifa Shen, Hui Dou and Xiaogang Zhang*

In this paper, a flexible film electrode was prepared by depositing graphene nanosheets on carbon nanotube paper as a self-standing electrode for high-performance electrochemical capacitors. The composite film has a layered structure, where carbon nanotubes were efficiently intercalated in the layer of graphene nanosheets. The hierarchical structure of graphene nanosheet/carbon nanotube paper electrode shows lower resistance for ions and electron transport. The unique electrode exhibits high-rate capability and long-term cycling ability. A quasi-rectangular shape of CV curve can still be maintained even at a high scan rate of 10 V s^{-1}. The capacitance decay was only 6.9% after 10000 cycles at a current density of 6.4 mA cm^{-2}.

Introduction

Recently, the applications of portable and flexible devices have come to fruition, for instance, devices like flexible touch screens and solar cells have become daily essentials.[1] Such breakthroughs have dramatically stimulated the development of related technologies, in particular the design and construction of energy-storage devices, one of the most important devices for human prosperity and health.[2, 3] Electrochemical capacitors are high-power energy-storage systems,[4-8] where charges are stored in the interface of electrolyte and electrode material through rapid and reversible adsorption/desorption of ions.[9-11] Much effort has also been made to develop thin-film supercapacitors with high capacity, light weight and flexibility.[12, 13] Theoretically, the two-dimensional (2D) extension of thin-film supercapacitors could substantially reduce the deformation resistance from the vertical direction, ultimately making the entire device thin, flexible, and easy to fold and twist. The diffusion distance of electrolyte ions in thin-film supercapacitor would also be shortened than their counterparts.

Graphene, a two-dimensional monolayer of sp^2-bonded carbon atoms, has attracted increasing attention in recent years, mainly due to its extraordinarily high electrical and thermal conductivities, great mechanical strength, large specific surface area, and potentially low manufacturing cost.[14-17] The intrinsic capacitance of single-layer graphene reaches *ca.* 21 μF cm^{-2} when the entire surface area is used.[18] Graphene film materials derived from graphite oxide (GO) and other carbon-based materials have exhibited excellent properties in various aspects, including high specific capacitance, long cycle stability, energy density, and power density. However, recent efforts have been predominately focused on developing novel electrode materials for thin-film supercapacitors, including reduced graphene oxide

film (462 μF cm^{-2}), polystyrene-based hierarchical porous carbon (28.7 μF cm^{-2}), active carbon (10 μF cm^{-2}) and carbon fabric (1 mF cm^{-2}).[19-24] However, studies aiming to further improve the area capacitance of thin-film supercapacitors are much less[25-28]. It is highly desirable to develop a facile method to prepare new graphene based two-dimensional materials for capacitors. Graphene-based electrodes offer higher densities owing to tight stacking of graphene sheets, which can prevent the ions from accessing the surface area and limit performance at high power.[17, 29-31] Liu *et al.* successfully prepared a new graphene foam/carbon nanotube hybrid film for use as efficient flexible electrode materials in asymmetric supercapacitor devices.[31] Therefore, a major challenge with graphene-based electrodes is developing novel structures that allow access to the surface area by incorporating sufficient porosity, utilizing spacers such as carbon spheres between graphene sheets to increase the spacing distance, which increase the capacitance of graphene electrodes by 70% in aqueous electrolyte. Dryfe *et al.* and Zhu *et al.* both successfully prepared a graphene on carbon cloth *via* an electrophoretic deposition process for use as efficient flexible electrode materials in supercapacitor devices.[16,27] However, highly irreversible agglomeration and precipitation of the graphene and poor capacitive behavior of these hybrid fibers rendered them far away from the ideal candidates for commercial purposes.

Herein, we demonstrate a facile method to fabricate an ultralight and highly conductive graphene nanosheets/carbon nanotube paper (GN/CNTP) composites as high-rate free-standing flexible electrodes for electrochemical capacitors. Highly conductive carbon nanotube papers (CNTP) are chosen as a flexible three-dimensional conductive substrate, can serve as an effective "spacer" to prevent the restacking of graphene nanosheets. Owing to interaction of π-π and functional groups between graphene oxide and carbon nanotubes, few-layer

graphene nanosheets are deposited on the both surfaces of carbon nanotube paper, inhibiting irreversible agglomeration and precipitation of graphene nanosheets. The final nanocomposites exhibited a capacity of 18.1 mF cm^{-2} according to the discharge curve at a current density of 3.2 mA cm^{-2}. This result indicates that this kind of composite design provides guidelines for fabricating electrode architectures to enhance electrochemical performances for supercapacitor.

Results and Discussion
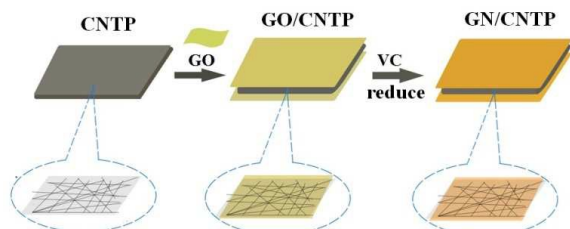
Scheme 1 Illustration of the synthesis of graphene nanosheets/ carbon nanotube paper.

Scheme 1 shows the illustration of fabrication the few-layer GN/CNTP for supercapacitor electrodes through a two-step process. A typical GN/CNTP composite electrode (Fig. 1a) can be prepared by immersing a pie of carbon nanotube paper (Fig. 1b) in a suspension of GO (6 mg mL^{-1}). Owing to interaction of π-π and functional groups between graphene oxide and carbon nanotubes, graphene nanosheets are deposited on the surface of carbon nanotube paper.[14, 32] The resulting graphene nanosheets/carbon nanotube paper composite film is then immersed in ascorbic acid (VC) solution (10 mg mL^{-1}) overnight and subsequently heated at 60 °C for 2 h. During this step, GO sheets are reduced to form graphene on the surface of carbon nanotube paper. [33]
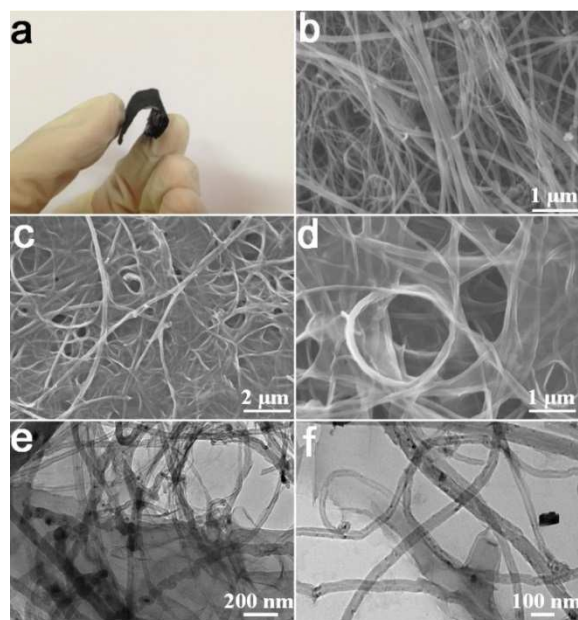
Fig. 1 (a) digital photograph of GN/CNTP, (b) SEM images of CNTP, (c, d) SEM images and (e, f) TEM images of stacked GN/CNTP at different magnifications.

Fig.1a shows the images of GN deposited on CNTP, in which GN and CNTP have formed integrated films. Fig.1b

shows that the CNTP overlap to appear as a fabric. The SEM images (Fig. 1c and d) of GN/CNTP clearly exhibit that GN has been successfully deposited on the surface of CNTP. The GN are well adhered to the both sides of the CNTP. Each CNTP is sandwiched between graphene nanosheets (Fig. 1e and f). This layer-by-layer (LBL) structure alleviates agglomeration of 2D carbon nanomaterials and maximizes the utilization of the surface of the graphene nanosheets to guarantee the permeation of electrolyte ions. The CNT layers can be served as well-defined porous spacer that not only prevent graphene film restackingbut provide sufficient separation between the wrinkled graphene film to faciliate electrolyte ions transfer.
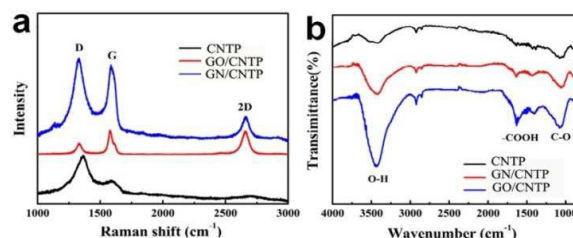
**Fig. 2** Raman (a) and FT-IR (b) spectra of CNTP, GO/CNTP and GN/CNTP.

The chemical structure of pure CNTP, GO/CNTP and GN/CNTP was further investigated by Raman. The Raman spectrums of pure CNTP, GN/CNTP, or GO/CNTP have two prominent bands around 1340 cm^{-1} and 1580 cm^{-1}, assigned to the D and G bands of carbon, respectively. The G band is related to graphitic carbon and the D band is associated with the structural defects or partially disordered structures of graphitic domains.[34-36] The I_D/I_G ratio provides a sensitive measure of the disorder and crystallite size of the graphitic layers.[37] The I_D/I_G value of GO/CNTP was calculated to be 0.75, while that of GN/CNTP was 1.04. This result indicates that the oxidized areas of GO sheets were partly restored upon reduction with VC, forming small conjugated domains. The higher I_D/I_G ratio indicates a high proportion of disorder in GN (the defects associated with edge surface and vacancies of graphene nanosheets), which are beneficial for electrochemical capacitance.[38] The Raman spectra of pure CNTP and GO/CNTP are different, implying that their components with different structure, mainly owing to GO films depositing.
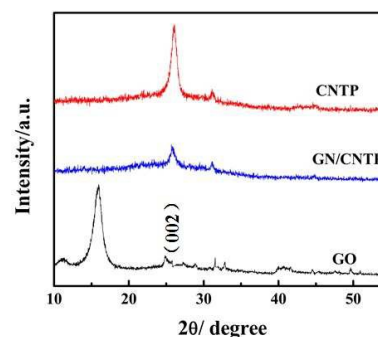
Fig.3 XRD patterns of CNTP, GN/CNTP and GO.

Fourier transform infrared spectrometry (FT-IR) was used to identify the functional groups of CNTP, GO/CNTP and GN/CNTP. As shown in Fig. 2b, the most characteristic features in the FTIR spectrum of GN are adsorption bands corresponding to C=O stretching at 1,721 cm^{-1}, O-H vibration

at 1,412 cm^{-1}, and a broad and intense O-H stretching at 3,400 cm^{-1}. After reduction, the bands of the -OH at 3,420 and 1,412 cm^{-1} were significantly reduced and that of -C=O groups at 1,721 cm^{-1} disappeared due to reduction of the oxygen group in GN. The powder X-ray diffraction (XRD) pattern of as-prepared GO，CNTP and GN/CNTP is shown in Figure 3. The diffraction peaks of CNTP at around 26° is attributed to the (002) diffraction peaks of graphite.[39, 40] The (002) diffraction peak of GO is much less intense than that of CNTP because the graphite structure is exfoliated by Hummer method. The (002) diffraction peak of GN/CNTP is much less intense than that of CNTP but stronger than that of GO because CNTP have intercalated between the graphene layers.[41]
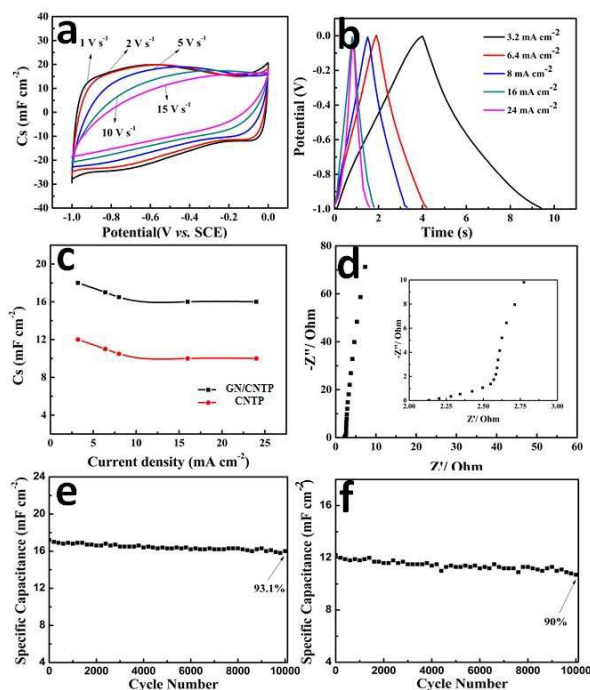
Fig. 4 (a) CV curves of GN/CNTP composites, (b) The charge/discharge profiles of GN/CNTP composites, (c) Plots of Cs of GN/CNTP s at various current densities, (d) Nyquist plots with a magnification for the high-frequency region in the inset. (e) Cycling stability of GN/CNTP upon charging/discharging at a current density of 6.4 mA cm^{-2}. (f) Cycling stability of pure CNTP upon charging/discharging at a current density of 6.4 mA cm^{-2}.

To investigate the electrochemical performance of the obtained GN/CNTP as an electrode material for supercapacitors, they were evaluated by cyclic voltammetry (CV) and galvanostatic charge/discharge measurements in a three-electrode system. An identical GN/CNTP composite film was directly used as the working electrodes without binders or conducting additives. The representative CV curves of the electrode in 6M KOH aqueous solution over the range of -1.0~0 V (Fig. 4a) at different scan rates, are close to the capacitive curve shape expected, especially at low scan rates. With increase of scan rate, the rectangular curve shape of the sample remains, even up to 10 V s^{-1}. The CV curves of GN/CNTP remained rectangular as the potential scan rate increased from 1 to 10 V s^{-1}, indicating good charge propagation at electrode/electrolyte interfaces following the mechanism of electric double-layer capacitors.[42] This high power property is ascribed to their high conductivity and structural/textural merits. The abundant opened CNTs favors the access of ions to the active surface, faciliating fast charge transfer. The results

demonstrate that the GN/CNTP film displayed improved rate capability.

The discharge curves of GN/CNTP measured at current densities in the range of 3.2~24.0 mA cm^{-2} show straight lines in the region of -1-0 V. The gravimetric specific capacitance for the three-electrode cell was obtained from the galvanostatic charge/ discharge curves as:

$$C_{single} = \frac{I \cdot t}{m_s \cdot V}$$

where m_s (g) is the mass of the working electrode, I (A) is the current density, t (s) is the discharge time and V (V) is the discharge voltage range. The specific capacitance (Cs) of GN/CNTP was calculated to be 18.1 mF cm^{-2} according to the discharge curve (Fig. 4b) at a current density of 3.2 mA cm^{-2}. In comparison, the GN/CNTP prepared from 6.0 mg mL^{-1} GO dispersion was coated on carbon nanotube paper and its amount is sufficient to completely fill the surface of carbon nanotube paper. However, as C$_{GO}$ decreased to 4.0 or 2.0 mg mL^{-1}, a sufficient amount of GO was formed to fully fill the surface of carbon nanotube paper. Actually, the specific capacitances of the GN/CNTP ECs were measured to be approximately identical to C$_{GO}$ because of the same amount of GO content in their electrodes. The capacitance retention ratio of GN/CNTP with a slight decrease at various charge/discharge current densities is shown in Fig. 4c. When the current density was further increased to a higher value of 24.0 mA cm^{-2}, a high C$_s$ of 16.2 mF cm^{-2} was still achieved and maintains 80 % compared to the initial capacitance. This high power stability with the GN/CNTP is ascribed to their conductivity[43] and their unique structural/ textural features. Electrochemical impedance spectroscopy (EIS) is carried out to prove that the short diffusion path of GNs/CNTP for electrolyte ions enhances ion transport kinetics. The resulting Nyquist plots exhibit inconspicuous Warburg curve, reflecting the short ion diffusion path in the electrode. At low frequencies, the nearly vertical behavior indicates that the surface area of the internal structure of GNs/CNTP electrode is wetted by the electrolytes. The abundant opened CNTP favors the access of ions to the active surface, making the charges transfer easier. These results reflect that the GN/CNTP has a high rate capability. The C$_s$ value of our GN/CNTP (18.1 mF cm^{-2} at the current density of 3.2 mA cm^{-2}) is at least one order of magnitude higher than those of the high-rates based on other carbon materials such as onion-like carbon (1.7 mF cm^{-2} at a scan rate of 1.0 V s^{-1})[44] and laser-scribed graphene (3.67 mF cm^{-2} at the current density of 36.3 μA cm^{-2}),[45] reduced graphene oxide film[17] (462 μF cm^{-2}), polystyrene-based hierarchical porous carbon[18] (28.7 μF cm^{-2}), active carbon[19] (10 μF cm^{-2}) and carbon fabric[20] (1 mF cm^{-2}). This is mainly because our GN/CNTP has graphene nanosheets and CNTs. Moreover, the cycle life is an important requirement for supercapacitor and the capacitance retention as a function of cycle number is shown for GN/CNTP in Fig. 4e. Even after charging-discharging for 10 000 cycles at a current density of 6.4 mA cm^{-2}, the capacitive retention is still as high as 93.1 %. In comparison, the cycling stability of pure CNTP is presented in Fig. 4f, which demonstrates an outstanding cycling stability with 90 % capacity remaining after 10000 continuous cycles.

Conclusions

In summary, we have proposed a simple layer-by-layer approach for construction of 2D planar ultrathin GN and CNTP as a flexible electrode for supercapacitors. This 2D planar architecture allows the formation of an efficient electrical

double layer and the utilization of the maximum active surface area of GN. The CNTP as a porous physical spacer could enhance the electrical conductivity and reduce the agglomeration of GN along the out-of-plane axis. Electrochemical tests show that a quasi-rectangular shape of CV curve can still maintained even at 10 V s^{-1}. The capacitance loss was only 6.9% after 10000 cycles at a current density of 6.4 mA cm^{-2}. These promising results demonstrate such a relatively easy-synthesis, low-cost, and macroscopic-scale electrode materials have great potential in the fabrication of high-class supercapacitor devices for practical applications.

Experimental section

Methods

Preparation of GO GO was prepared *via* the oxidation of natural graphite powder according to a modified Hummers' method.[46] In brief, 1.5 g graphite powder was added into a mixture of 10 mL 98% H_2SO_4, 1.25 g $K_2S_2O_8$, and 1.25 g P_2O_5, and the solution was maintained at 80 °C for 4.5 h. The resulting pre-oxidized product was washed with water and dried in a vacuum oven at 50 °C. After it was mixed with 60 mL 98% H_2SO_4 and then slowly added 7.5 g $KMnO_4$ at a temperature below 20 °C, followed by adding 125 mL H_2O. After 2 h, additional 200 mL H_2O and 10 mL 30% H_2O_2 were slowly added into the solution to completely react with the excess $KMnO_4$. After 10 minutes, a bright yellow solution was obtained. The resulting mixture was washed with diluted HCl aqueous (1/10 v/v) solution and H_2O. The graphite oxide was obtained after drying in a vacuum oven at 30 °C. 200 mg graphene oxide was dispersed in 200 mL deionized water by sonication and then centrifuged to get graphene oxide solution.

Preparation of GN/CNTP Typically, carbon papers (1.5 cm × 1 cm, mass per unit area 1.67 mg cm^{-2}) were immersed in a GO suspension (C_{GO} = 6.0 mg mL^{-1}). Then the system was kept for 24 h. Subsequently, the carbon paper containing GO films were transferred into a freeze-drying vessel (-50 °C, 20 Pa) and freeze-dried for 12 h. Then, the freeze-dried carbon nanotube paper containing GO films were transferred to plastic tubes with a diameter of 1.3 cm containing 3.0 mL of 10.0 mg mL^{-1} VC, the reaction system was allowed to remain without any interruption overnight and then heated at 60 °C for 2 h. After cooling down to room temperature naturally, the GN/CNTP composite films were rinsed with deionized water for several times.

Characterization

Scanning electron microscopy (SEM) and transmission electron microscopy (TEM) were carried out with a JEOL JSM-6380LV FESEM and JEOL JEM-2010, respectively. Powder X-ray diffractions (XRD) was studied by Bruker D8 Advance X-ray diffractometer using Cu Kα radiation. Fourier transform infrared spectrometry(FT-IR)measurements were recorded on a Nicolet750. The Raman spectra were measured by using a Jobin Yvon HR800 confocal Raman system with a 632.8 nm diode-laser excitation on a 300 S mm^{-1} line grating at RT.

Electrochemical measurements

Cyclic voltammetry (CV) and galvanostatic charge/discharge behaviors of GN/CNTP electrodes were investigated on a CHI 660A electrochemical workstation (Shanghai Chenhua, China) in a conventional three-electrode system with 6 M KOH aqueous solution as the electrolyte. Platinum foil and a saturated calomel electrode (SCE) were used as counter and reference electrodes. The working electrodes were prepared by mixing active material (1 cm^2). After coating the film on foamed Ni grids (1cm×1cm), the electrodes were dried at 60 °C for several hours before pressing under a pressure of 10 MPa.

Notes and references

Jiangsu Key Laboratory of Material and Technology for Energy Conversion, College of Material Science and Engineering,Nanjing University of Aeronautics and Astronautics, Nanjing, China. Fax: +86 025 52112626; Tel: +86 025 52112918; E-mail: azhangxg@163.com

1. X. Lee, T. T. Yang, X. Li, R. J. Zhang, M. Zhu, H. Z. Zhang, D. Xie, J. Q. Wei, M. L. Zhong, K. L. Wang, D. H. Wu, Z. H. Li and H. W. Zhu, *Appl. Phys. Lett.*, 2013, **102**.

2. J. L. Liu, M. H. Chen, L. L. Zhang, J. Jiang, J. X. Yan, Y. Z. Huang, J. Y. Lin, H. J. Fan and Z. X. Shen, *Nano Lett*, 2014, **14**, 7180-7187.

3. J. L. Liu, J. Sun and L. A. Gao, *J Phys Chem C*, 2010, **114**, 19614-19620.

4. C. G. Liu, Z. N. Yu, D. Neff, A. Zhamu and B. Z. Jang, *Nano Lett*, 2010, **10**, 4863-4868.

5. J. J. Yoo, K. Balakrishnan, J. S. Huang, V. Meunier, B. G. Sumpter, A. Srivastava, M. Conway, A. L. M. Reddy, J. Yu, R. Vajtai and P. M. Ajayan, *Nano Lett*, 2011, **11**, 1423-1427.

6. C. Z. Meng, C. H. Liu, L. Z. Chen, C. H. Hu and S. S. Fan, *Nano Lett*, 2010, **10**, 4025-4031.

7. L. B. Hu, M. Pasta, F. La Mantia, L. F. Cui, S. Jeong, H. D. Deshazer, J. W. Choi, S. M. Han and Y. Cui, *Nano Lett*, 2010, **10**, 708-714.

8. G. Y. Xu, B. Ding, P. Nie, L. F. Shen, J. Wang and X. G. Zhang, *Chem-Eur J*, 2013, **19**, 12306-12312.

9. P. Simon and Y. Gogotsi, *Nat Mater*, 2008, **7**, 845-854.

10. J. R. Miller and P. Simon, *Science*, 2008, **321**, 651-652.

11. A. K. Mondal, B. Wang, D. W. Su, Y. Wang, S. Q. Chen, X. G. Zhang and G. X. Wang, *Mater Chem Phys*, 2014, **143**, 740-746.

12. C. Z. Wu, X. L. Lu, L. L. Peng, K. Xu, X. Peng, J. L. Huang, G. H. Yu and Y. Xie, *Nat. Commun.*, 2013, **4**.

13. M. Kaempgen, C. K. Chan, J. Ma, Y. Cui and G. Gruner, *Nano Lett.*, 2009, **9**, 1872-1876.

14. D. S. Yu and L. M. Dai, *J Phys Chem Lett*, 2010, **1**, 467-470.

15. Q. Wu, Y. X. Xu, Z. Y. Yao, A. R. Liu and G. Q. Shi, *Acs Nano*, 2010, **4**, 1963-1970.

16. D. H. Wang, R. Kou, D. Choi, Z. G. Yang, Z. M. Nie, J. Li, L. V. Saraf, D. H. Hu, J. G. Zhang, G. L. Graff, J. Liu, M. A. Pope and I. A. Aksay, *Acs Nano*, 2010, **4**, 1587-1595.

17. H. R. Byon, S. W. Lee, S. Chen, P. T. Hammond and Y. Shao-Horn, *Carbon*, 2011, **49**, 457-467.

18. J. L. Xia, F. Chen, J. H. Li and N. J. Tao, *Nat Nanotechnol*, 2009, **4**, 505-509.

19. H. S. Teng, Y. J. Chang and C. T. Hsieh, *Carbon*, 2001, **39**, 1981-1987.

20. Y. C. Cao, M. Zhu, P. X. Li, R. J. Zhang, X. M. Li, Q. M. Gong, K. L. Wang, M. L. Zhong, D. H. Wu, F. Lin and H. W. Zhu, *Phys. Chem. Chem. Phys.*, 2013, **15**, 19550-19556.

21. F. C. Wu, R. L. Tseng, C. C. Hu and C. C. Wang, *J. Power Sources*, 2005, **144**, 302-309.

22. W. Xing, S. Z. Qiao, R. G. Ding, F. Li, G. Q. Lu, Z. F. Yan and H. M. Cheng, *Carbon*, 2006, **44**, 216-224.

23. Z. H. Li, D. C. Wu, Y. R. Liang, F. Xu and R. W. Fu, *Nanoscale*, 2013, **5**, 10824-10828.

24. C. W. Huang, C. H. Hsu, P. L. Kuo, C. T. Hsieh and H. S. Teng, *Carbon*, 2011, **49**, 895-903.

25. J. Yan, T. Wei, B. Shao, F. Q. Ma, Z. J. Fan, M. L. Zhang, C. Zheng, Y. C. Shang, W. Z. Qian and F. Wei, *Carbon*, 2010, **48**, 1731-1737.

26. J. Yan, Z. J. Fan, T. Wei, W. Z. Qian, M. L. Zhang and F. Wei, *Carbon*, 2010, **48**, 3825-3833.

27. Z. Q. Niu, L. Zhang, L. Liu, B. W. Zhu, H. B. Dong and X. D. Chen, *Adv. Mater.*, 2013, **25**, 4035-4042.

28. X. H. Cao, Y. M. Shi, W. H. Shi, G. Lu, X. Huang, Q. Y. Yan, Q. C. Zhang and H. Zhang, *Small*, 2011, **7**, 3163-3168.

29. Y. Wang, Z. Q. Shi, Y. Huang, Y. F. Ma, C. Y. Wang, M. M. Chen and Y. S. Chen, *J. Phys. Chem. C*, 2009, **113**, 13103-13107.

30. M. D. Stoller, S. J. Park, Y. W. Zhu, J. H. An and R. S. Ruoff, *Nano Lett.*, 2008, **8**, 3498-3502.

31. J. L. Liu, L. L. Zhang, H. B. Wu, J. Y. Lin, Z. X. Shen and X. W. Lou, *Energ Environ Sci*, 2014, **7**, 3709-3719.

32. Q. Cheng, J. Tang, J. Ma, H. Zhang, N. Shinya and L. C. Qin, *Phys Chem Chem Phys*, 2011, **13**, 17615-17624.

33. J. Chen, K. X. Sheng, P. H. Luo, C. Li and G. Q. Shi, *Adv. Mater.*, 2012, **24**, 4569-4573.

34. D. Graf, F. Molitor, K. Ensslin, C. Stampfer, A. Jungen, C. Hierold and L. Wirtz, *Nano Lett*, 2007, **7**, 238-242.

35. V. Lee, L. Whittaker, C. Jaye, K. M. Baroudi, D. A. Fischer and S. Banerjee, *Chem Mater*, 2009, **21**, 3905-3916.

36. X. B. Cao, D. P. Qi, S. Y. Yin, J. Bu, F. J. Li, C. F. Goh, S. Zhang and X. D. Chen, *Adv Mater*, 2013, **25**, 2957-2962.

37. S. Sampath, A. N. Basuray, K. J. Hartlieb, T. Aytun, S. I. Stupp and J. F. Stoddart, *Adv Mater*, 2013, **25**, 2740-2745.

38. K. Gao, Z. Shao, X. Wu, X. Wang, Y. Zhang, W. Wang and F. Wang, *Nanoscale*, 2013, **5**, 5307-5311.

39. D. S. Zhang, T. T. Yan, L. Y. Shi, Z. Peng, X. R. Wen and J. P. Zhang, *J Mater Chem*, 2012, **22**, 14696-14704.

40. Z. Y. Guo, J. Wang, F. Wang, D. D. Zhou, Y. Y. Xia and Y. G. Wang, *Adv Funct Mater*, 2013, **23**, 4840-4846.

41. D. Zhang, T. Yan, L. Shi, Z. Peng, X. Wen and J. Zhang, *J Mater Chem*, 2012, **22**, 14696.

42. Z. S. Wu, Y. Sun, Y. Z. Tan, S. B. Yang, X. L. Feng and K. Mullen, *J Am Chem Soc*, 2012, **134**, 19532-19535.

43. Z. Q. Niu, W. Y. Zhou, J. Chen, G. X. Feng, H. Li, W. J. Ma, J. Z. Li, H. B. Dong, Y. Ren, D. A. Zhao and S. S. Xie, *Energy Environ. Sci.*, 2011, **4**, 1440-1446.

44. D. Pech, M. Brunet, H. Durou, P. H. Huang, V. Mochalin, Y. Gogotsi, P. L. Taberna and P. Simon, *Nat. Nanotechnol.*, 2010, **5**, 651-654.

45. M. F. El-Kady, V. Strong, S. Dubin and R. B. Kaner, *Science*, 2012, **335**, 1326-1330.

46. D. C. Marcano, D. V. Kosynkin, J. M. Berlin, A. Sinitskii, Z. Z. Sun, A. Slesarev, L. B. Alemany, W. Lu and J. M. Tour, *Acs Nano*, 2010, **4**, 4806-4814.

RSC Advances Accepted Manuscript

Table of contents entry
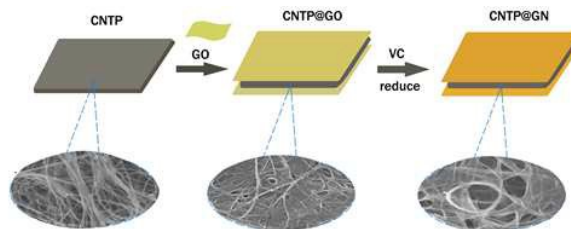
Graphene nanosheets/carbon nanotube paper for supercapacitor: We present an ultralight weight and highly conductive graphene nanosheets/carbon nanotube paper composites as high-rate free-standing flexible electrodes for electrochemical capacitors. Highly conductive carbon nanotube papers are chosen as a flexible three-dimensional conductive substrate, can serve as an effective "spacer" to prevent the restacking of graphene nanosheets.